

**OPEN ACCESS**

## SQUID magnetometry for the cryoEDM experiment—Tests at LSBB

To cite this article: S Henry *et al* 2008 *JINST* **3** P11003

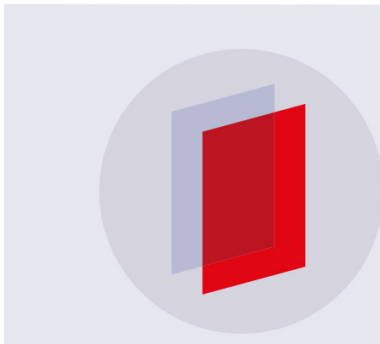
View the [article online](#) for updates and enhancements.

### Related content

- [A Simple Strong SQUID](#)  
Keiz Murata, Terumi Kawai, Yasuyuki Sato *et al.*
- [CryoEDM: a cryogenic experiment to measure the neutron Electric Dipole Moment](#)  
C A Baker, S N Balashov, V Francis *et al.*
- [Magnetic state of Nb\(1-7nm\)/Cu30Ni70 \(6nm\) superlattices revealed by Polarized Neutron Reflectometry and SQUID magnetometry](#)  
Yu. Khaydukov, R. Morari, D. Lenk *et al.*

### Recent citations

- [A SQUID magnetometry system for a cryogenic neutron electric dipole moment experiment](#)  
S. Henry *et al*
- [Characterisation of superconducting capillaries for magnetic shielding of twisted-wire pairs in a neutron electric dipole moment experiment](#)  
S. Henry *et al*
- [Tracking geomagnetic fluctuations to picotesla accuracy using two superconducting quantum interference device vector magnetometers](#)  
S. Henry *et al*



**IOP | ebooks™**

Bringing you innovative digital publishing with leading voices to create your essential collection of books in STEM research.

Start exploring the collection - download the first chapter of every title for free.

RECEIVED: *July 10, 2008*REVISED: *October 16, 2008*ACCEPTED: *October 29, 2008*PUBLISHED: *November 14, 2008*

# SQUID magnetometry for the cryoEDM experiment

## — Tests at LSBB

---

**S. Henry,<sup>a\*</sup> H. Kraus,<sup>a</sup> M. Malek,<sup>a</sup> V.B. Mikhailik<sup>a</sup> and G. Waysand<sup>b</sup>**

<sup>a</sup>*University of Oxford, Department of Physics, Denys Wilkinson Building,  
Keble Road, Oxford, OX1 3RH, U.K.*

<sup>b</sup>*Laboratoire Souterrain à Bas Bruit de Rustrel-Pays d'Apt (LSBB),  
Université de Nice Sophia-Antipolis,  
La Grande Combe, 84400 Rustrel, France  
E-mail: s.henry1@physics.ox.ac.uk*

**ABSTRACT:** High precision magnetometry is an essential requirement of the cryoEDM experiment at the Institut Laue-Langevin, Grenoble. We have developed a SQUID system for this purpose, however tests done in Oxford have been limited by the noisy electromagnetic environment inside our laboratory, therefore we have tested a smaller version of our prototype system in the very low noise environment at LSBB, Rustrel, France. We have studied the crosstalk between an array of parallel pick-up loops — where the field generated by a current in one loop is detected by the others. We monitored the magnetic field in the LSBB for over twelve hours; and after correcting these data for SQUID resets, and crosstalk, we compare it to the published values from nearby geomagnetic observatories. We have also measured the noise spectrum of our system and studied the effect that heating one of the pick-up loops into its conducting state has on the other, parallel loops.

**KEYWORDS:** Control and monitor systems online; Cryogenic detectors; Analysis and statistical methods.

---

\*Corresponding author.

---

## Contents

<b>1. Introduction</b>	<b>1</b>
1.1 CryoEDM	1
1.2 Tests of our prototype system at LSBB	3
<b>2. Setup at LSBB</b>	<b>3</b>
<b>3. Data corrections</b>	<b>4</b>
3.1 SQUID resets	6
3.2 Crosstalk	8
3.3 Calibration	10
<b>4. Magnetometry measurements</b>	<b>12</b>
4.1 The difference between signals in two pick-up loops	13
<b>5. Noise spectra and resolution</b>	<b>16</b>
<b>6. Heating pick-up loops to destroy superconductivity</b>	<b>20</b>
<b>7. Conclusions</b>	<b>23</b>

---

## 1. Introduction

### 1.1 CryoEDM

The cryoEDM experiment is a search for the electric dipole moment (EDM) of the neutron based at the Institut Laue-Langevin (ILL) in Grenoble [1]. The limit on this parameter of  $|d_n| < 2.9 \times 10^{-26} e \cdot \text{cm}$  set by the previous phase of the experiment (nEDM) [2, 3], is one of the most significant results in determining the scale of T violation. CryoEDM aims to improve this limit to  $\sim 10^{-28} e \cdot \text{cm}$ , which will cover the range predicted by the majority of supersymmetric theories. The experiment works by storing a large number of ultra cold neutrons (UCN), and measuring any change in their spin precession frequency when the external electric field is reversed. If the neutron has a non-zero EDM, we will measure a change in the precession frequency.

As the neutron has a significant magnetic dipole moment, a change in the magnetic field during a measurement cycle could give a false positive signal. To avoid this we need to monitor the magnetic field to a very high resolution. The nEDM phase of the experiment did this very successfully using atomic mercury spectroscopy [4]. However to significantly improve the sensitivity it will be necessary to greatly increase the number of UCN. CryoEDM will do this using a new UCN source which exploits the properties of superfluid helium [5]; but as this operates at cryogenic temperatures, the mercury magnetometer cannot be used. Therefore we have developed a suitable SQUID

magnetometer system to replace it. This will be the first use of SQUID magnetometry to directly measure the magnetic field in a neutron EDM experiment.<sup>1</sup>

The neutron spin precession frequency  $\nu$  in an electric field  $E$  and magnetic field  $B$  is given by

$$\hbar\nu = 2dE \pm 2\mu B \quad (1.1)$$

where  $d$  is the electric dipole moment and  $\mu$  the magnetic dipole moment. From this we can show that the frequency shift caused by an electric dipole moment of  $10^{-28}$  e·cm in an electric field of  $\pm 50$  kV·cm<sup>-1</sup> is the same as that caused by a change in the magnetic field of 0.17 fT. To achieve this sensitivity will require  $\sim$ 70,000 measurements (several months of data taking) and a magnetometer resolution of  $\sim 10^{-13}$  T for each measurement.<sup>2</sup>

During a neutron measurement we will use the SQUIDs to track any drift in the magnetic field between measurements of the precession frequency for different applied electric fields. Each precession frequency measurement is averaged over  $\sim$ 130 s — limited by the lifetime of the neutrons in the storage volume.

Whereas the mercury magnetometer measured the volume averaged magnetic field; SQUIDs are only sensitive to relative changes in the flux through pick-up loops. We intend to record the signals from multiple pick-up loops to extrapolate the magnetic field in the region of interest. This is complicated by the presence of high voltage electrodes used to generate the electric field. As SQUIDs are easily damaged by static, the pick-up loops must be located a safe distance from the electrodes. To achieve the necessary extrapolation we will use a total of twelve SQUID readout channels. It is important for magnetic field reconstruction that we understand the crosstalk between these.

SQUIDs can achieve noise levels of  $\sim$ fT·Hz<sup>-1/2</sup> above 10 Hz. At low frequencies the noise increases as  $1/f$ . A typical performance reported in [7] is

$$\left( \frac{2 \times 10^{-14}}{\sqrt{f}} \right) \text{THz}^{-1/2}. \quad (1.2)$$

Integrating this from 1/130 s (the time for which the neutrons are stored and the precession frequency measured) to 10 Hz gives a resolution of  $1.3 \times 10^{-13}$  T. From this we conclude it is feasible to use SQUIDs as magnetometers in a neutron EDM experiment at this sensitivity. However we stress that this is only an order of magnitude estimate. The precise bandwidth required for a cryoEDM measurement cannot be defined at this stage. We may wish to monitor the magnetic field over much longer periods, but we will take the average field over the duration of each measurement (in effect operating with lower upper and lower frequency bounds than those given above), although it will be necessary to monitor the SQUID output at a higher frequency to ensure any drift is within acceptable limits.

There is still a great deal of work to be done before we can measure the neutron EDM to our targeted precision. In this paper we report work done to develop a SQUID magnetometer to monitor

---

<sup>1</sup>Reference [6] describes a proposal to use SQUIDs to measure the precession frequency of <sup>3</sup>He atoms in a neutron EDM experiment.

<sup>2</sup>This is one possibility. We may achieve the same sensitivity with fewer longer magnetic field measurements and a higher resolution (by taking the average over several precession frequency measurements).

the magnetic field in the cryoEDM experiment. The next stages will be to run the magnetometry system in a suitably shielded cryostat at ILL; to develop the signal processing and data analysis techniques; and to use it (with the rest of the cryoEDM apparatus) to measure the neutron EDM.

## 1.2 Tests of our prototype system at LSBB

Our system uses SQUID sensors supplied by Supracon<sup>3</sup> with readout electronics from Star Cryoelectronics.<sup>4</sup> Woven cables to read out the SQUIDs have been made to our design by TekData.<sup>5</sup> We have designed and made our own pick-up loops, and written our own software, to control the system, and for data acquisition and analysis.

Our laboratory, located in central Oxford, is unfortunately not a suitable site to test such a system. Therefore we have tested a smaller version of the cryoEDM system at the Laboratoire Souterrain à Bas Bruit (LSBB) in Rustrel, 100 km north of Marseille, a former control centre for the French ground-based nuclear missile arsenal [8]. At the heart of this laboratory, there is a room (called the capsule) shielded by 1cm thick steel, resting on shock absorbers, surrounded by 500 m of rock. In this environment we expect our system to be limited only by fluctuations of the magnetic field of the Earth. The environment at LSBB is monitored by a set of STS2 seismometers (5 underground, one on the top), and the magnetic field is monitored using the 3 axes *[SQUID]2* system [9].<sup>6</sup>

In the cryoEDM experiment, we need to use the signals from a series of pick-up loops to extrapolate the magnetic field in the volume where the neutrons are stored. In these tests, we have measured the signals in several loops, mounted coaxially with their planes parallel, and used these data to study the crosstalk between loops.

The data discussed in this paper were taken during two field trips to LSBB, one in March and the other in September 2006. In the March trip we monitored the magnetic field with three SQUIDs connected to parallel pick-up loops; one loop was fitted with a heater to allow us to heat the loop above its superconducting transition. In September we carried out further tests using a five channel system, where two of the SQUIDs were connected in series to a single pick-up loop; and some measurements were carried out with an additional lead shield around the loops.

In the following section we describe the setup we installed at LSBB; we then outline the data analysis process to correct for SQUID resets and crosstalk, and calibrate the system; then we compare this to measurements from nearby geomagnetic observatories and discuss the significance of the difference between the signals measured with different pick-up loops. In the final sections we give the noise spectra and describe the effect of heating one of the loops into its conducting state.

## 2. Setup at LSBB

In March 2006 we carried out some preliminary tests using three SQUIDs; two of these (labelled #3 and #4) were connected to two 24 mm diameter loops made from a single turn of 0.127 mm diameter NbTi wire, wound on the same former. The other SQUID (labelled #5) was connected to a

<sup>3</sup>Supracon AG, Wildenbruchstr. 15, D-07745 Jena, Germany

<sup>4</sup>Star Cryoelectronics, 25A Bisbee Court, Santa Fe, NM-87508-1412, U.S.A.

<sup>5</sup>TekData, Westport House, Federation Road, Burslem, Stoke-on-Trent, ST6 4HY, U.K.

<sup>6</sup>Shielding QUalified for Ionosphere Detection with SQUID.

**Table 1.** Details of the pick-up loops attached to the SQUIDs. Channels 1 and 2 were not used during the March measurements.

Setup	SQUID	Loop diameter (mm)	Distance from calibration coil (mm)	Heater	Wire diameter (mm)
March	#3	24	46	Yes	0.127
	#4	24	46	No	0.127
	#5	34	56	No	0.25
September	#1	30	59	No	0.25
	#2	30	73	Yes	0.25
	#3	30	59	No	0.25
	#4	30	73	No	0.25
	#5	Connected to the same loop as SQUID 4			

34 mm diameter loop made from 0.25 mm NbTi wire, positioned 10 mm below the other loops. All loops were mounted parallel to the ground to measure the vertical component of the magnetic field. The wires between the loops and SQUID input terminals were twisted together. A heater was attached to the twisted wire pair connected to SQUID 3 to allow us to heat the loop into its conducting state, while the other loops remained superconducting.

In September 2006 we installed a five channel system at LSBB. This had four pick-up loops consisting of 30 mm diameter loops of 0.25 mm diameter NbTi wire. Two loops were wound on each of two formers separated by 14 mm. One loop was connected to the inputs of two SQUIDs (connected in series), giving five channels in total.

In both setups, a calibration coil was mounted away from the pick-up loops. A photograph of the September setup is shown in figure 1. Table 1 lists the details of the loops and shows which one is connected to each SQUID.

The SQUIDs and pick-up loops were lowered into a helium dewar located inside the LSBB capsule. The SQUID preamplifier and control electronics were mounted next to the cryostat, connected to a data acquisition system and computer (located outside of the capsule) by 15 m long screened cables, and a fibre-optic link.

The capsule is not a true Faraday cage as the shielding was incomplete and the cables running inside were unfiltered. All mains power was kept outside, with only DC power lines to control the equipment by the cryostat. The output of the SQUID electronics ( $\pm 10$  V) was recorded using a 12 bit Aurora 14 transient recorder.

The September setup was designed to allow a lead shield (a cylinder open at one end) to fit over the pick-up loops, calibration coil and part of the SQUID sensors. This shield reduced the magnetic field by a factor of around 30, and was used to assess the noise level (discussed in section 5). The shield was not installed for the calibrations and magnetometry measurements as the compact dimensions of the shield caused the field from the calibration coils to be distorted.

### 3. Data corrections

In section 4 we will present our measurement of the magnetic field over two periods of around

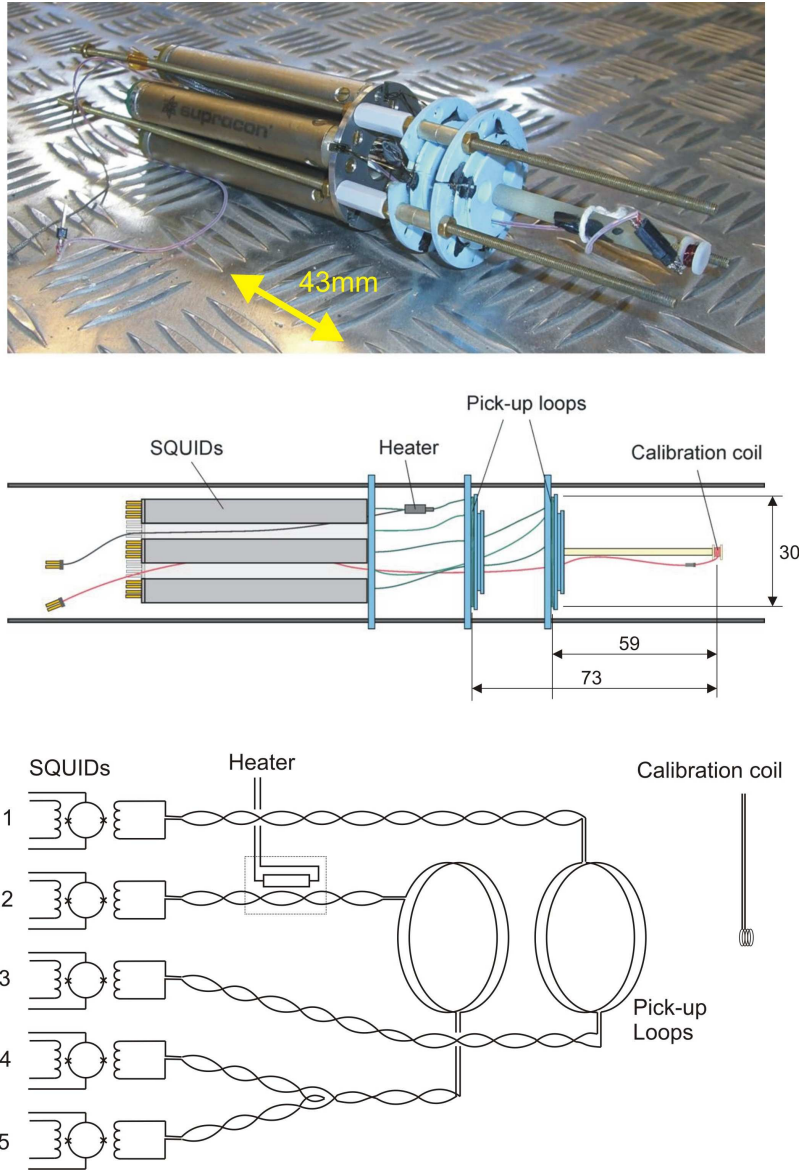


**Figure 1.** Photograph, drawing and schematic of the SQUIDs, pick-up loops and calibration coil used for the measurements carried out in September. The dimensions shown are in mm. The SQUIDs are connected by twisted wire pairs to pick-up loops wound on plastic formers, made to accommodate two loop diameters (in the September setup all loops were wound on the larger diameter). A heater was installed on one twisted wire pair, and a calibration coil was mounted away from the loops. The setup here is pictured horizontally, but it was mounted on a dipstick with the calibration coil at the bottom and lowered vertically into a dewar of liquid helium.

twelve hours (for March and September). But first, we explain how these data were acquired and analysed.

The measurements were made by recording a frame of 8192 or 16384 samples (referred to as an *event*) using a transient recorder every 2 or 4 seconds. The timebase (sampling interval) was  $100\ \mu\text{s}$ , giving a total sample of 0.82 or 1.63 s. A step function was applied to the calibration

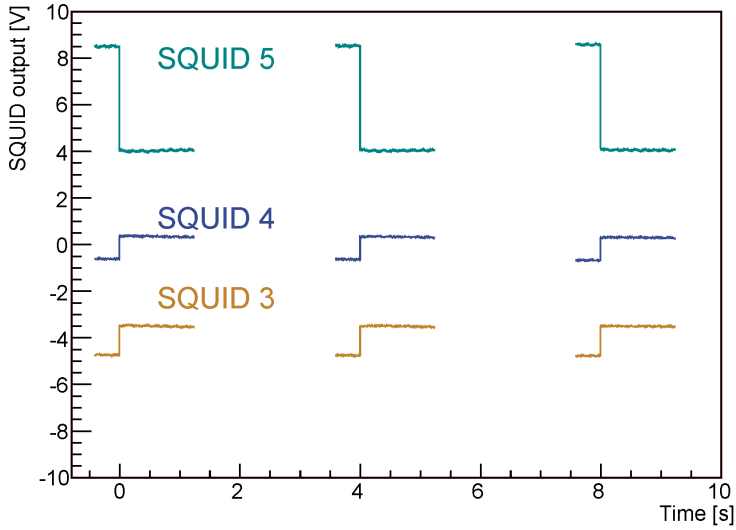


**Figure 2.** Three consecutive events recorded in the March dataset. As the SQUIDs are only sensitive to relative changes in the magnetic flux the absolute scale is arbitrary. The step is due to the calibration signal, which produces an average field of 0.13 nT through the loop connected to SQUIDs 3 and 4, and 0.21 nT through the loop connected to SQUID 5.

coil 1/4 of the way through each sample to allow us to monitor the calibration throughout the measurement. Figure 2 shows three events from the March dataset as an example. SQUIDs are only sensitive to relative changes in the magnetic flux, therefore the absolute scale shown on plots of our data is arbitrary and we frequently offset the plotted data to improve clarity.

The data plotted in the graphs in this section were calculated by taking the average over 95% of the pretrigger region (before the calibration step). To extract a value for the magnetic field strength from this *baseline* value, we need to first correct the data for SQUID resets, crosstalk between channels, and then convert it to nT. These steps are now explained in turn.

### 3.1 SQUID resets

The SQUIDs are run in a flux-locked loop where the current applied to the feedback coil is adjusted to keep the flux through the SQUID loop constant, and the output signal is the voltage on the feedback line. Whenever the output reaches the limit of its range ( $\pm 10$  V), the SQUID resets, jumping an integer number of flux quanta to a value close to 0 V [10]. These jumps can be seen on the uncorrected data in figure 3.

The SQUIDs can be run in different ranges by changing the resistor in the feedback line. In the *low* range ( $\sim 0.1$  V $\Phi_0^{-1}$ ) only one SQUID reset was recorded over a 14 hour measurement. However in this range the drift over a short time was limited by the resolution of the data acquisition system. Therefore it was preferable to operate the SQUIDs in the *medium* range ( $\sim 1$  V $\Phi_0^{-1}$ ), and correct the SQUID resets using software. The SQUIDs were in *medium* range for all the tests discussed in this paper unless otherwise stated.

The software corrects the data by adding or subtracting a fixed value whenever the baseline changes abruptly. For this method to work, the SQUID must reset by the same number of flux

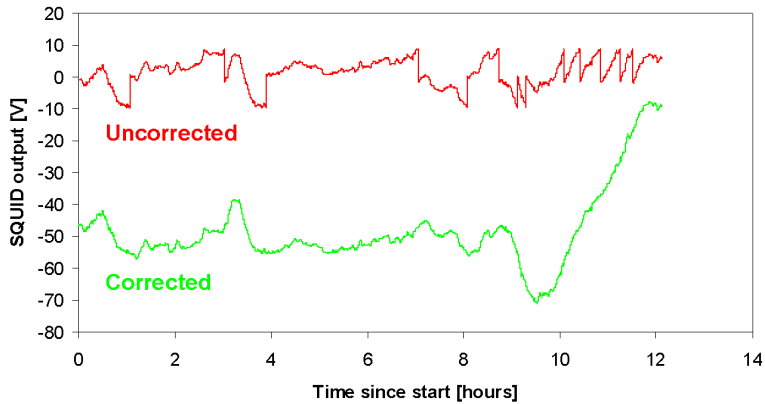


**Figure 3.** The uncorrected SQUID output (ranging from -10 to +10V), and the data corrected for resets. The absolute value is arbitrary and the corrected curve has been offset for clarity.

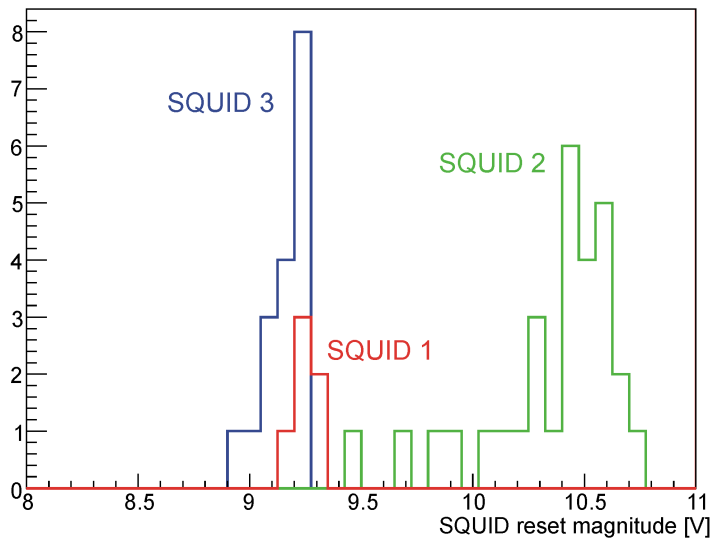


**Figure 4.** A histogram showing the distribution of values for the magnitude of abrupt changes in the baseline between two events, attributed to SQUID resets, (from the September dataset). Each SQUID resets by an integer number of flux quanta. The spread of values is due to the drift of the baseline over the measurement period; as this is less than one flux quantum, we assume all resets as the same magnitude and we correct for this by adding or subtracting a fixed value at each reset.

quanta each time. Figure 4 shows a histogram of the magnitude of the resets for the September data. As the spread of values for each SQUID is less than one flux quantum (measured as 1.91, 1.66 and  $2.34 \pm 0.06$  V for SQUIDs 1, 2 and 3), this seems to be the case. The spread of values is due to the drift in the signal between adjacent events.

A study of events containing a reset (such as that shown in figure 5) gave a smaller range of values. These events were cut out of the sample before running the correction program as the presence of a reset often meant the baseline was not calculated correctly. The corrected data are shown in figure 3.

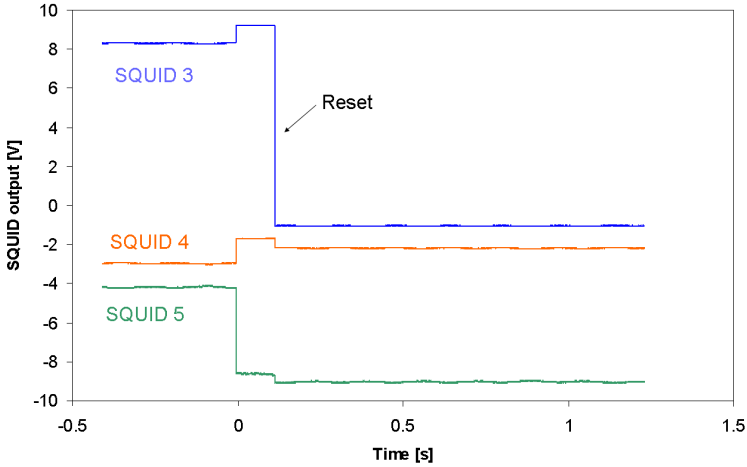


**Figure 5.** The output of all three SQUIDs. The jump at  $t=0$  is due to a signal from the calibration coil. At  $t=0.11$  s SQUID 3 resets from  $\sim 10$  to  $\sim 0$  V, and the change in the feedback current produces a crosstalk signal in channels 4 and 5.

### 3.2 Crosstalk

When two or more pick-up loops are located close together there will be a small crosstalk between them [10]. In reference [11] ter Brake et al. explain how this can be eliminated by applying the feedback to the input circuit (instead of directly to the SQUID). In this paper we explain how to correct crosstalk effects using software. Crosstalk arises because the current induced in a loop by a change in the magnetic flux, will itself generate a field. In a simple model, the change in the magnetic flux  $\Delta\Phi$  through a SQUID input circuit is given by

$$\Delta\Phi = \Delta\Phi_{\text{ext}} + I_i L_T + I_f M_{\text{fi}} \quad (3.1)$$

where  $I_i$  is the supercurrent circulating in the input loop,  $L_T$  is the total inductance of the input circuit,  $I_f$  is the current applied to the feedback coil, and  $M_{\text{fi}}$  is the mutual inductance between the feedback and input coils. When the external applied flux  $\Delta\Phi_{\text{ext}}$  rises (or falls),  $I_i$  will fall (or rise) such that  $\Delta\Phi = 0$ .

The first two terms of equation (3.1) give the flux through the pick-up loop. The last term gives the extra flux through the SQUID input coil due to the feedback current. This contributes only a few percent and in a single channel magnetometer it can be ignored as  $I_f \propto I_i$ , so it simply increases the effective inductance of the input loop.

When we have two or more pick-up loops in close proximity, the change in flux through pick-up loop  $n$  is given by

$$\Delta\Phi_n = \Delta\Phi_{\text{ext}} + (I_i)_n L_T + \sum_m (I_i)_m M_{nm} \quad (3.2)$$

where the sum is over all other pick-up loops ( $m \neq n$ ),  $(I_i)_n$  is the current flowing through loop  $n$ , and  $M_{nm}$  is the mutual inductance between loops  $n$  and  $m$ .<sup>7</sup> In this case the current  $I_i$  flowing around

<sup>7</sup>The feedback current term is not present as this expression is for just the flux through the pick-up loop instead of the whole input circuit.

**Table 2.** The signal induced in each SQUID in the March setup due to a positive reset (-10 to 0 V) in another SQUID.

Reset SQUID	$\Delta V$ induced by the SQUID reset		
	SQUID 3	SQUID 4	SQUID 5
3		0.47	0.42
4	0.58		0.40
5	0.30	0.39	

one loop affects the  $\sum (I_i)_m M_{nm}$  term for the next loop. To keep  $\Delta\Phi=0$  for this loop,  $I_i$  for this loop will change, so we have a crosstalk signal. This is best illustrated by looking at the signal on all channels when one SQUID resets, which is illustrated in figure 5.

When SQUID 3 resets from  $\sim 10$  V to 0 V, the feedback current changes from  $10V/R_f$  to 0 (where  $R_f$  is the resistor on the feedback line). To keep  $\Delta\Phi=0$ ,  $I_i$  will increase. This keeps the total flux through the SQUID input circuit constant, but causes a small change in the flux through the pick-up loop, which is picked up by the neighbouring loops. To keep the flux through pick-up loop 4 constant (being parallel to 3), the input current around this loop must change, giving a crosstalk signal. The voltage steps in each SQUID induced by resets in the other SQUIDs are listed in table 2 for the March setup.

A SQUID reset will cause a change in the current through the pick-up loop of

$$\Delta I_i = \frac{\Delta I_f M_{fi}}{L_T}. \quad (3.3)$$

In the medium range  $R_f = 100$  k $\Omega$  giving a change in the feedback current of  $\Delta I_f = 100$   $\mu$ A; we estimate the input circuit inductance as  $L_T = 435$  nH.<sup>8</sup> The data sheet gives  $M_{fi} = 7.4$  nH, but this is reduced when a pick-up loop is attached to the input. During the September tests we used the setup with two SQUIDs connected to the same loop to measure this. By changing the current applied to the feedback loop of one SQUID, and measuring the signal on the other, we determined that  $M_{fi} = 4.3$  nH. It will be even lower for loops attached to a single SQUID, where the total inductance of the input circuit is less.

Substituting these numbers into equation (3.3) gives  $\Delta I_i = 520$  nA. Given this and the crosstalk currents, in theory we can calculate the mutual inductances. In practice this is complicated as we must consider the crosstalk between each loop and every other loop, and as we do not know the inductances with any accuracy, we can only give a rough estimate. From the values in table 2 we estimate the mutual inductances between loops are typically  $M_{nm} \sim 100$  nH.

Using the data in table 2 we can rescale the measured voltage of each SQUID channel to correct for this crosstalk by using equation (3.4)

$$\mathbf{V}^{\text{corrected}} = \mathbf{V}^{\text{noresets}} - \mathbf{X} \cdot \mathbf{V}^{\text{resets}} \quad (3.4)$$

where each  $\mathbf{V}^{\dots}$  parameter is a vector containing the voltages for all SQUIDs; and  $\mathbf{X}$  is a matrix containing the data in table 2 divided by the magnitude of each reset ( $\sim 10$  V).  $\mathbf{V}^{\text{noresets}}$  has had

<sup>8</sup>Taken from the Supracon data sheet, the SQUID input inductance is 350 nH, and we calculate pick-up loop inductance as 85 nH [12] giving  $L_T = 435$  nH.

the SQUID reset jumps removed (the “corrected” line in figure 3),  $\mathbf{V}^{\text{resets}}$  contains the output with resets (the “uncorrected” line in figure 3). For the March setup, we can write this as

$$\begin{bmatrix} V_3^{\text{corrected}} \\ V_4^{\text{corrected}} \\ V_5^{\text{corrected}} \end{bmatrix} = \begin{bmatrix} V_3^{\text{noresets}} \\ V_4^{\text{noresets}} \\ V_5^{\text{noresets}} \end{bmatrix} - \begin{bmatrix} 0 & 0.065 & 0.037 \\ 0.045 & 0 & 0.041 \\ 0.041 & 0.045 & 0 \end{bmatrix} \cdot \begin{bmatrix} V_3^{\text{resets}} \\ V_4^{\text{resets}} \\ V_5^{\text{resets}} \end{bmatrix} \quad (3.5)$$

We could in principle correct the crosstalk for the five channels in the September data using a  $5 \times 5$  matrix. In practice this is difficult because (as explained above) two SQUIDs were connected to the same pick-up loop. In this case a reset in one SQUID invariably triggered a flux jump in the second and the two effects could not be separated. Therefore, when taking the magnetometry data shown in section 4, we ran only three SQUIDs. In this case the crosstalk correction matrix was

$$\begin{bmatrix} 0 & 0.024 & 0.004 \\ 0.009 & 0 & 0.009 \\ 0.033 & 0.040 & 0 \end{bmatrix} \quad (3.6)$$

In order to assess the accuracy of this correction, we plot the difference between the signals from two SQUIDs. As the pick-up loops were all mounted parallel to each other, a negligible distance apart, we would expect (to a first approximation) that the two SQUIDs will show the same signal, and the difference would be zero. This is shown for SQUIDs 3 and 5 in figure 6. As this curve is roughly proportional to the magnetometry signal from both SQUIDs (shown in figure 7), the main reason for the difference is due to the limited accuracy of the calibration of one or both magnetometers (discussed further in sections 3.3 and 4.1). However we can see by comparing the plot before and after the crosstalk correction, that this correction gives a noticeable improvement. The top plot (before the crosstalk correction) is characterised by abrupt changes whenever one of the other SQUIDs resets.

### 3.3 Calibration

The first jump shown on the event in figure 5 was produced by sending a current step of  $62.5\mu\text{A}$  to the calibration coil. The calibration coil was made from 200 turns of copper wire on a 1 mm former. As the distance between the coil and the pick-up loops was larger than the size of the coil we treat it as a magnetic dipole. This assumption was supported by numerical modelling of the coil. Thus, we calculate a magnetic field signal (for  $i_c = 62.5\mu\text{A}$ ) of 0.13 nT for SQUIDs 3 and 4, and 0.21 nT for SQUID 5 (in the March setup). As the construction of the coil and the measurements of its dimensions are not perfect we expect an error of  $\sim 10\%$ . By measuring the average voltage jump on each SQUID due to this signal, we calculate the values in table 3.

In the March setup, the loops attached to SQUIDs 3 and 4 were identical, but the twisted wire pair connected to SQUID 3 was longer. This increased the inductance of the loop and explains why SQUID 3 showed a lower signal than SQUID 4. A heater was also attached to the input circuit of SQUID 3, this consisted of a resistor, around which the twisted wire pair was coiled; this also increased the inductance of the circuit.<sup>9</sup> The loop attached to SQUID 5 had approximately twice the area of the loops attached to SQUIDs 3 and 4 (see table 1), so the signal is correspondingly higher.

<sup>9</sup>A heater was also attached to SQUID 2 in the September setup, which shows a larger signal than the other loops. However in this case the twisted wire pair was not coiled so tightly around the heater, so we would not expect a significant increase in the inductance. The heater is described in more detail in section 6.

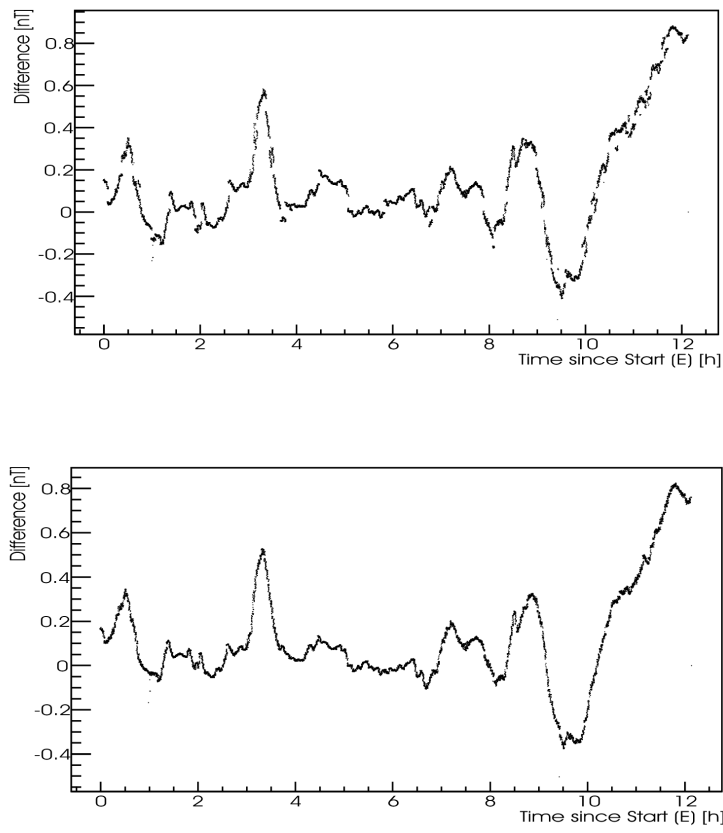


**Figure 6.** The difference between signals from SQUIDs 3 and 5, before (top) and after (bottom) correcting the crosstalk. This follows roughly the same pattern as the magnetic field measurement shown in figure 7 so it appears the largest error is in the calibration.

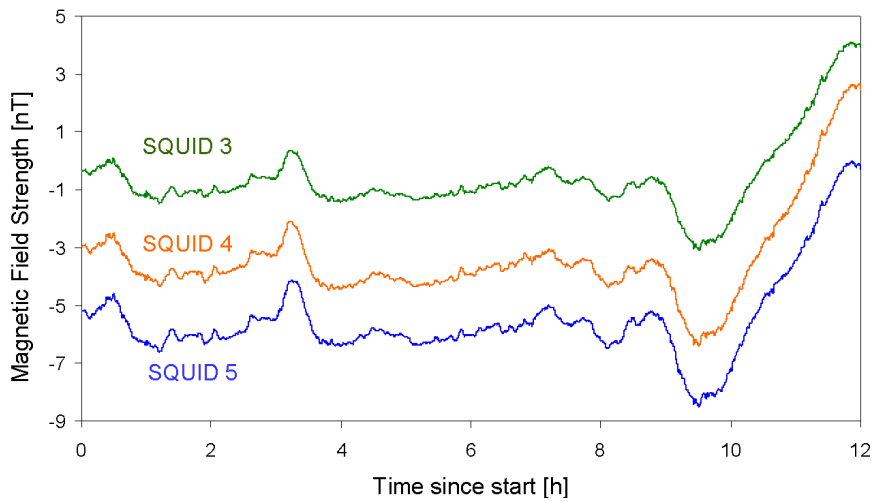


**Figure 7.** The magnetic field measured by all three SQUIDs after the corrections and calibrations. The traces have been offset for clarity.

**Table 3.** The response of each SQUID to a signal from the calibration coil. The errors show the RMS spread of values.

SQUID	Signal response [VnT <sup>-1</sup> ]	
	March setup	September setup
1		$-8.1 \pm 0.3$
2		$12.9 \pm 0.9$
3	$7.5 \pm 0.4$	$-11.1 \pm 0.2$
4	$9.8 \pm 0.4$	$-5.2 \pm 0.5$
5	$-21.0 \pm 0.5$	$-5.2 \pm 0.6$

In the September setup all the loops were wound on formers of the same diameter, therefore we would not expect the loop area to differ by more than a few percent. The different magnitudes of calibration signal are likely to be due to a combination of factors including the loop size, length of the twisted-wire-pairs and the mutual inductance between loops. As SQUIDs 4 and 5 were connected to the same loop, the signals in these SQUIDs differed only by 1.1%, the magnitude expected due to the variation of the input coupling between SQUIDs. As the loop had a total inductance of 785 nH, instead of 435 nH, the magnitude is correspondingly lower compared to the loops connected to only one SQUID.

#### 4. Magnetometry measurements

After removing the SQUID resets, correcting the crosstalk and converting the voltage to nanotesla, the resulting magnetic field strength recorded during the 12 hour March measurement is shown in figure 7. To be sure this really is a measurement of the magnetic field in the laboratory, we compared our results with published geomagnetic data. The Earth's magnetic field shows fluctuations  $\sim 10$  nT each day due to currents in the ionosphere. It is influenced by many factors and these fluctuations can be quite different at different locations. There is no single geomagnetic observatory close to Rustrel. Therefore we compare our data to the vertical component of the magnetic field measured by three observatories at: Chambon la Forêt (in France), Ebro (Spain), and Fürstenfeldbruck (Germany) [13]. This is shown in figure 8, with the field measured by SQUID 5. The geomagnetic observatories monitor all three components of the Earth's magnetic field to 0.1 nT precision using fluxgate magnetometers, recording data points every minute.

We carried out a simple linear extrapolation of these measurements to Rustrel, assuming the geomagnetic field is given by

$$B = a + b \times \text{latitude} + c \times \text{longitude} \quad (4.1)$$

and calculating  $a$ ,  $b$  and  $c$  to fit the geomagnetic data at each data point. The observatories record the absolute field strength, but the data shown in figure 8 have been offset to show all lines at a scale which shows the fluctuations.

The result, as figure 8 shows, is an approximate match to our data. As the geomagnetic field shows significant regional variations, we would not expect anything better. The vertical component of the magnetic field recorded by Ebro shows significantly more variation than that recorded by

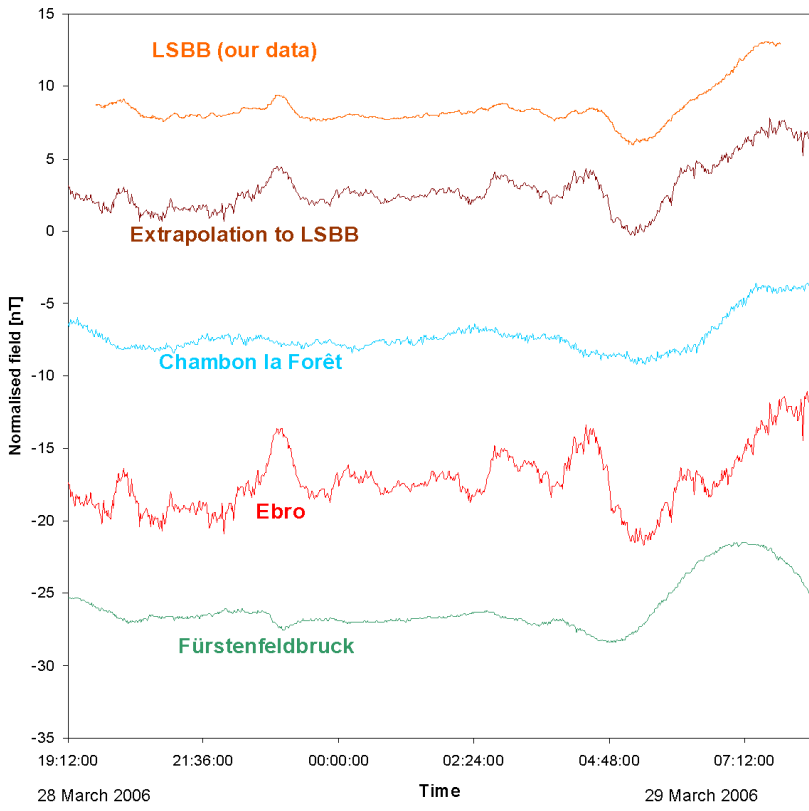


**Figure 8.** Fluctuations in the magnetic field measured at LSBB, with that measured by three geomagnetic observatories (to 0.1 nT precision). These show different patterns as fluctuations in the geomagnetic field on this scale vary between different locations. We plot a linear extrapolation of these data to Rustrel to compare with our measurement. A fixed value has been subtracted from each dataset to present the traces on the same scale, and the lines have been offset for clarity.

other observatories as due to its coastal location it is sensitive to currents induced in the Mediterranean Sea [14]. These are not present in our measurements at Rustrel, but they do share some features with the Ebro data which were not recorded by Chambon la Forêt and Fürstenfeldbruck; these are likely to be caused by ionospheric currents to the South.<sup>10</sup>

As the signal we measured is close to what we expect from the geomagnetic data we are confident that it is due to the Earth's magnetic field. The LSBB seismometers did not record any significant activity over this period.

#### 4.1 The difference between signals in two pick-up loops

Figure 6 shows the difference between the magnetometry signal measured by SQUIDs 3 and 5. As this curve is roughly proportional to the signal from either SQUID, this appears to be due to the imperfect calibration of the magnetometers. To make a more appropriate comparison we first

<sup>10</sup>We also note that on that day (29 March 2006) there was a partial solar eclipse, which produced a time and position dependent magnetic field signal as the shadow of the moon moved across the ionosphere [9], although this effect was small.

rescale one of the SQUID signals to fit the other. The magnetic field signal from SQUID 4, rescaled to fit SQUID 3,  $B_4^{(3)}$  is given by

$$B_4^{(3)} = \alpha B_4 + \beta \quad (4.2)$$

where  $B_4$  is the unscaled field (but corrected for SQUID resets and crosstalk) and  $\alpha$  and  $\beta$  are calculated to give the minimum  $\sum (B_4^{(3)} - B_3)^2$  (sum over all data points). The values of  $\alpha$  calculated for  $B_4^{(3)}$ ,  $B_5^{(3)}$  and  $B_5^{(4)}$  are 0.93, 1.16, 1.25. The difference between the scaled and the reference SQUID output is shown in figure 9 for all three SQUIDs.

Figure 9 shows the correlation is best between pick-up loops 3 and 5, and is a similar magnitude between 4 and 5. As these loops are wound on the same former, we conclude the magnetic field gradient between loops 3/4 and 5 is negligible, and the difference between the signals on each SQUID is mainly due to other factors.

The likely cause is pick-up of other (horizontal) components of the magnetic field in the twisted wire pairs, or if the pick-up loops are not perfectly aligned. The twisted wire pair from SQUID 3 passed through the heater, where it was wrapped around a resistor. It is likely the twisting is less than perfect at this point, causing it to pick up extra magnetic flux.

To test this hypothesis, figure 10 compares  $B_5^{(3)} - B_3$  with the value of the geographic north field component at Rustrel (extrapolated from the geomagnetic observatory data). The two lines match very well. We can make a rough estimate of the magnitude of the horizontal pick up from figure 11, which shows a side and end view of the pick up loops, with the calculated areas. From this diagram we expect the ratio of the signal due to the magnet field parallel to the loop, to that due to the field perpendicular to it to be  $\leq 4.2\%$ . The loop is unlikely to be folded such that the horizontal area is the maximum size calculated here, but this estimate neglects any pick-up in the twisted wire pair, and assumes the plane of the loop is perfectly horizontal, therefore we can only treat this as a rough estimate.

From figure 10 we can see that during our measurement, the North-South component of the geomagnetic field varied over a range of  $\sim 10$  nT, while the difference between our measurements  $B_5^{(3)} - B_3$  varied by  $\sim 0.4$  nT, the expected order of magnitude.

The data discussed so far in this section is from the March dataset. Doing the same analysis for a long measurement in the September dataset gives the plots shown in figure 12 and figure 13. This time, in addition to looking at the geomagnetic observatory data, we recorded the signals from the [SQUID]2 magnetometer. This monitors the field in three directions (vertical, north-south, and east-west) and gave a more accurate calibration than the extrapolated geomagnetic data. This analysis gives the same conclusion as that drawn from the March data.

We conclude this section with a short summary of the systematic errors on our measurement of the relative change in the vertical component of the magnetic field, and some rough estimates of their magnitude. We estimate the accuracy of the calibration is  $\sim 10\%$  and our comparison of the signals in two loops suggest this is about right. Pick-up of the horizontal component of the field due to misalignment is  $\sim 4\%$ . The largest crosstalk in this setup was  $\sim 80$  pT, but this is corrected to  $\sim 5\%$  accuracy reducing this effect to  $\sim 4$  pT. Correcting the SQUID resets will produce a cumulative error  $\propto \delta V_{\Phi_0} \sqrt{N}$  where  $\delta V_{\Phi_0}$  is the error on our measurement of the voltage difference

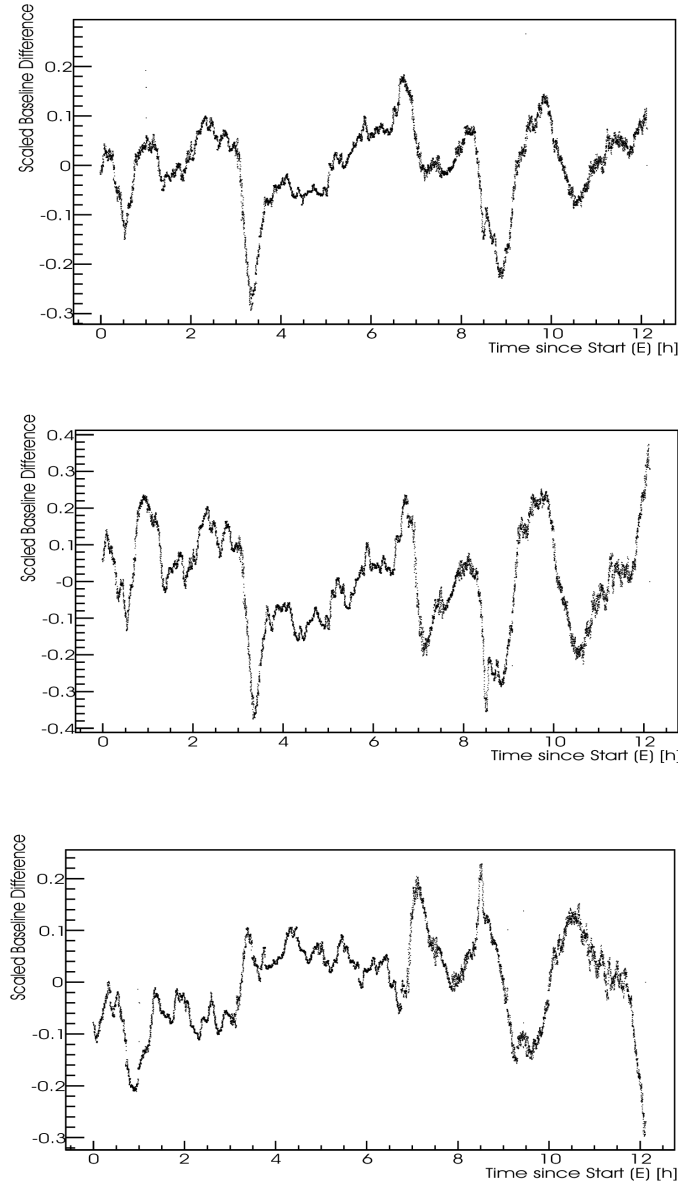


**Figure 9.** The difference between the rescaled and reference SQUID outputs (in nT), top  $B_3^{(5)} - B_5$ , middle  $B_3^{(4)} - B_4$ , bottom  $B_4^{(5)} - B_5$ .

corresponding to  $1\Phi_0$ , and  $N$  is the number of resets. This gives an effective drift over our 12 hour measurement of  $\sim 20$  pT.

In the following section we discuss in detail the resolution of the SQUID magnetometer. The intrinsic 1/f noise of the SQUID will cause the SQUID output to drift over a long time period. If this contribution is the same as that measured with a SQUID with shorted input, and if the noise spectrum shown in figure 14 for a bare SQUID continues to scale as  $1/\sqrt{f}$ , then we would expect the drift over 12 hours to be 32 fT.

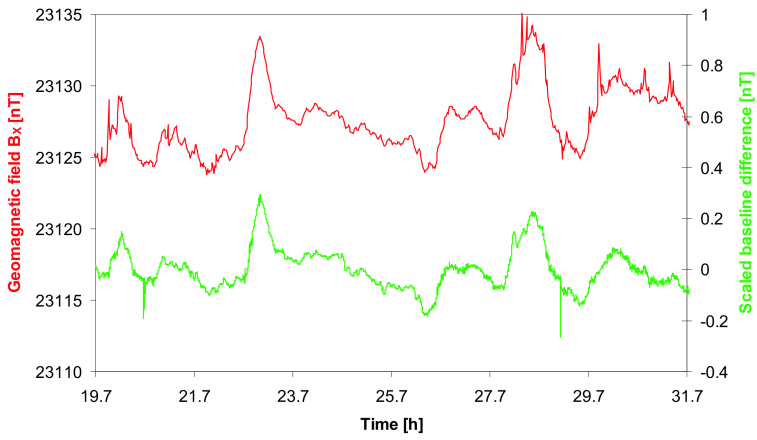


**Figure 10.** Top trace: a linear extrapolation of the X (geographic north) component of the magnetic field at Rustrel from the data measured at Chambon la Forêt, Fürstenfeldbruck, and Ebro geomagnetic observatories; bottom trace: the difference between the rescaled and reference SQUID baseline  $B_5^{(3)} - B_3$  (inverted to give the same polarity). As the two traces follow the same pattern it seems the dominant error is pick-up of the horizontal field.

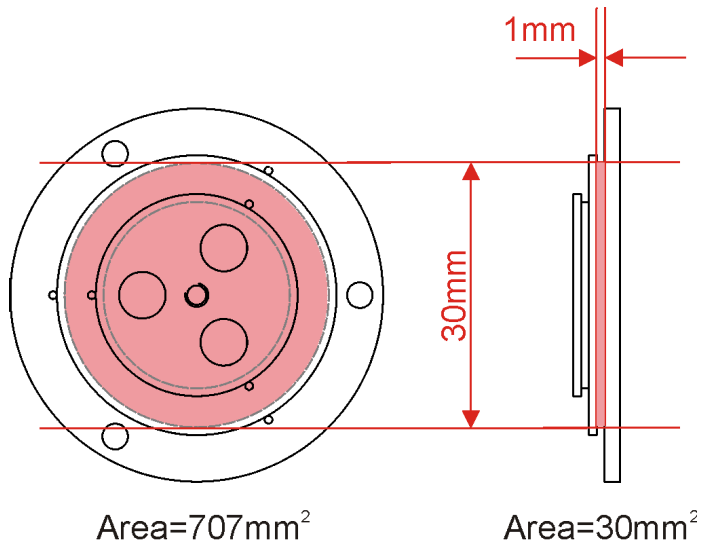


**Figure 11.** The pick-up loops are designed to measure the vertical component of the magnetic field. In this plane a 30 mm diameter loop has an area of  $707 \text{ mm}^2$ . The maximum possible horizontal area for the pick-up loop is  $30 \text{ mm}^2$ , (the actual area will depend on exactly how the wires lie). Therefore we predict a ratio of horizontal pick-up to vertical pickup of  $\leq 30/707 = 4.2\%$ .

## 5. Noise spectra and resolution

Figure 14 shows the noise spectra recorded during the September run. These were produced from  $\sim 80$  recorded baseline samples with 6 different timebases from  $1 \mu\text{s}$  to  $100 \text{ ms}$ . An 8-pole Butterworth filter was installed before the transient recorder and used to block any noise above the Nyquist frequency in these measurements. Two spectra were plotted using data taken with and without the lead shield in place.

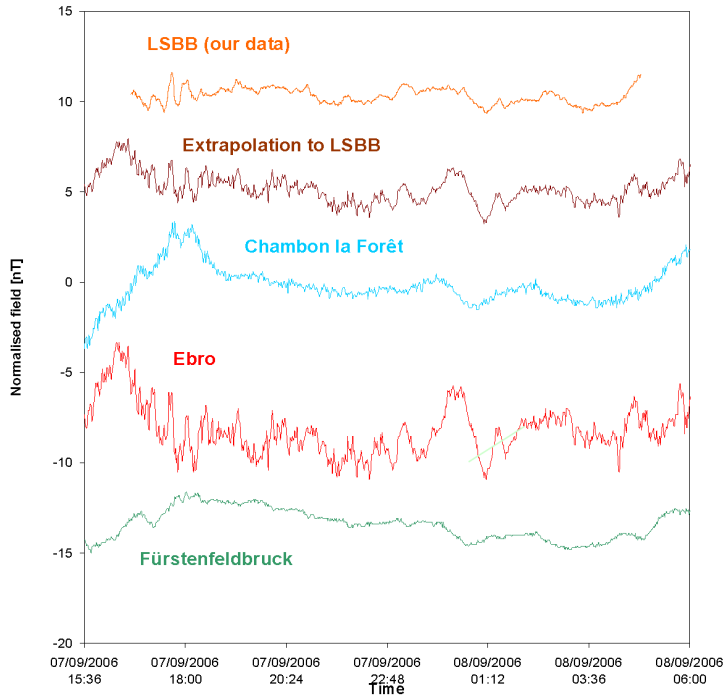


**Figure 12.** The magnetic field signal measured at LSBB in September, with that measured by the three geomagnetic observatories and a linear extrapolation of these data to Rustrel as was shown in figure 8.

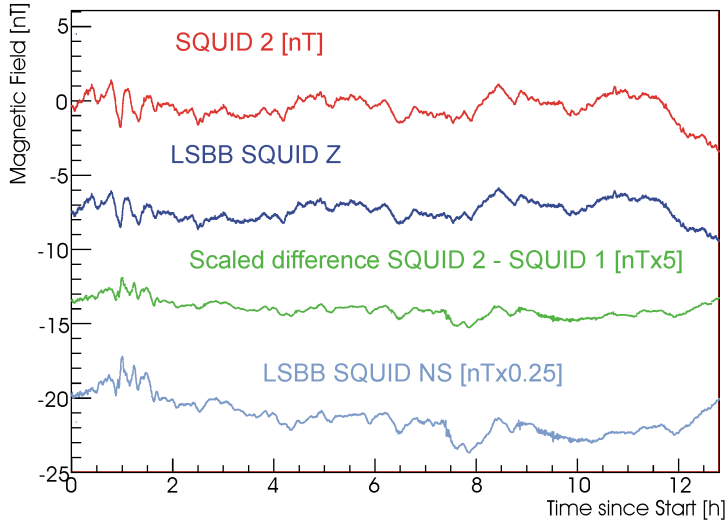


**Figure 13.** 12 hour magnetic field measurement taken during September 2006. The top two lines show the field measured by one of our SQUIDs (after all the corrections), and that measured by the permanent LSBB SQUID magnetometer (measuring the vertical field). The third line shows the scaled difference between the signals on two of our SQUIDs (multiplied by 5 to make the fluctuations visible), the bottom line shows the LSBB magnetometer for the North-South direction.

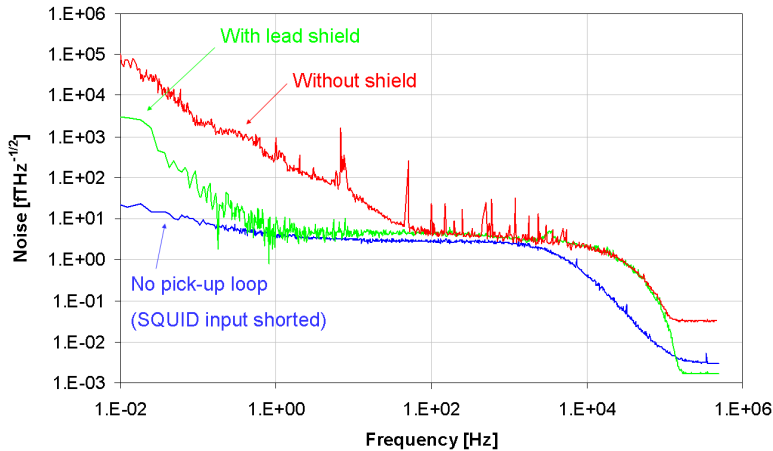


**Figure 14.** The noise spectra for our SQUID magnetometer (#1) recorded at LSBB with and without the superconducting shield. The spectrum measured for a bare SQUID with the pick-up loop replaced by a  $0\Omega$  short across the input terminals is also shown (converted to fT using the same calibration factor). The data points have been smoothed.

At high frequencies the intrinsic SQUID noise is greater than the magnetic field noise and the spectra are flat, until the noise drops off above the SQUID bandwidth. Below  $\sim 100$  Hz the unshielded spectrum shows the spectrum of the magnetic noise in the laboratory (this is the same level as that measured by the permanent SQUID magnetometer at LSBB [15]). There is a small peak at 50 Hz due to the field generated by the power cables. At lower frequencies the noise increases as  $1/f$ .

The shielded spectrum shows a flat white noise level of  $4.0 \text{ fT} \cdot \text{Hz}^{-1/2}$  above  $\sim 1$  Hz; below this it increases as the frequency falls, approximately as  $(4.9/f) \text{ fT} \cdot \text{Hz}^{-1/2}$ , although the lowest frequency points are even higher. This is the magnetic field noise, reduced by a factor  $\sim 30$  by the shield. Figure 14 also shows a noise spectrum measured in Oxford with an identical sensor, but with the pick-up loop replaced by a very short superconducting wire, shorting the input terminals on the SQUID chip (converted to fT using the same calibration factor). This shows the intrinsic noise of the SQUID, which is what we would measure with no external field fluctuations.<sup>11</sup> This gives a white noise of  $2.6 \text{ fT} \cdot \text{Hz}^{-1/2}$  above 1 Hz and  $(3.2/\sqrt{f}) \text{ fT} \cdot \text{Hz}^{-1/2}$  below this. Note that while the geomagnetic field shows an approximately  $1/f^2$  power spectrum (or  $1/f$  magnetic field spectrum), the SQUID power only rises as  $1/f$ .

We can calculate the FWHM resolution of the magnetometer,  $\delta B$ , by integrating the noise spectrum; as shown in equation (5.1),

$$\delta B = 2.35 \sqrt{\int_{\frac{1}{T}}^{f_{\max}} B_n^2 \, df} \quad (5.1)$$

where  $B_n(f)$  is the noise level at frequency  $f$  (in units of tesla per root hertz),  $f_{\max}$  is the bandwidth and  $T$  is the measurement time (which sets the lower frequency limit).

<sup>11</sup>There will be a small difference as the inductance of the input circuit is different, but as the pick-up loop inductance is only  $\sim 20\%$  of the total inductance this effect is small. This explains why the lines in figure 14 do not overlap perfectly at high frequency.

**Table 4.** The resolution of the magnetometer calculated from the noise spectra in figure 14 for a cut-off frequency of 10 Hz. The magnetometer resolutions (with and without the shield) were limited by fluctuations in the geomagnetic field, so these figures are an upper limit on the performance. The resolution calculated from the bare SQUID noise is what we could achieve in a better shielded environment (unless limited by other factors).

Measurement time [s]	80	8
Resolution (no shield)	14 pT	2.7 pT
Resolution (with shield)	570 fT	49 fT
Resolution from bare SQUID noise	27 fT	26 fT

Table 4 shows the resolutions calculated using equation 11 from the spectra in figure 14. With the shield in place, we derive a resolution of 0.57 fT for our setup for a cut-off frequency of 10 Hz, and a measurement time of 80 s (the longest time period covered by these noise spectra). If the geomagnetic spectrum continues to scale as  $1/f$  at lower frequencies, then we estimate we would measure a resolution of 0.73 pT for a measurement time of 130 s.

This is higher than our target of  $\leq 0.1$  pT for a 130 s measurement with 10 Hz cutoff. However we stress that this is merely the best we can demonstrate in this environment. It is limited by fluctuations in the Earth's magnetic field. We can estimate the resolution we could achieve with perfect magnetic shielding from the noise spectrum for the bare SQUID. This gives 27 fT for an 80 s measurement, which would increase to 28 fT for 130 s (noise scaling as  $1/\sqrt{f}$ ). In practice we are unlikely to achieve such a low resolution even with improved shielding, as there will always be some thermal magnetic noise due to the shielding materials. However as our target of 100 fT is 3-4 times this value, we believe it is achievable. This conclusion assumes that the geomagnetic field noise we measured is not masking another noise source. A further analysis of the noise measured by the two SQUIDs connected to the same loop supports this.

Figure 15 shows the noise spectrum for SQUID 4, (the one connected to the same loop as SQUID 5). This is significantly higher than SQUID 1 as it also receives the noise produced by SQUID 5; and the higher inductance of the two SQUID loop reduced the signal (so when converted to fT the noise level is higher). Using the procedure described in section 4.1 we calculated the scaled difference between the two SQUIDs for all events, and took the frequency spectrum of the result, which is also shown in figure 15. This is illustrated in figure 16 for two events.

In theory the magnetic field noise will give an identical signal in both SQUIDs, so the scaled difference spectrum should show the intrinsic noise of the two SQUIDs. In practice, at some frequencies, this difference was limited by the bit resolution of the transient recorder, so the line in figure 15 is only an upper limit. However it is encouraging to note that this spectrum does not increase so dramatically at low frequency, confirming our belief that this feature, which limits the resolution we demonstrated, is due to the external magnetic field.

To conclude this section, the best resolution we have demonstrated at Rustrel is 0.57 pT for a measurement time of 80 s and 10 Hz cutoff. This is less than our target of 0.1 pT, but this is limited by the magnetic environment. Even in the low noise environment at LSBB we still detect fluctuations in the Earth's magnetic field below 10 Hz. We have shown that these low frequency fluctuations are due to the magnetic field and not another noise source, as the frequency spectrum

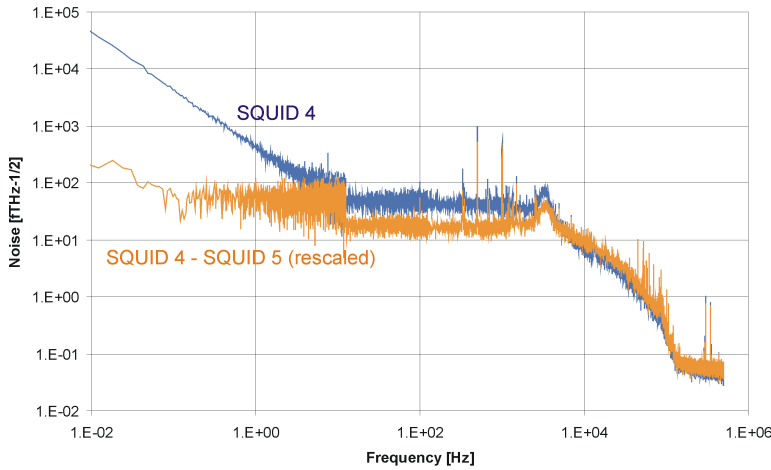


**Figure 15.** The noise spectrum for SQUID 4 (which was connected in series with SQUID 5 to the pick-up loop); together with the frequency spectrum of the scaled difference between the two samples (calculated using the procedure described in section 4.1). In this plot the data points are not smoothed so the boundaries between different datasets are visible. At the upper end of the lowest spectrum, the quantization noise of the transient recorder dominated. This is not the case for the higher frequency datasets, which were recorded with the filter preceding the transient recorder set to a higher gain. This gives rise to the apparent jump at 12 Hz.

of the scaled difference between the signals in two SQUIDs connected to the same pick-up loop did not rise so rapidly at low frequencies. If we could achieve the noise level equal to that measured with a SQUID with shorted input, then we could achieve a resolution of 27 fT (same measurement time and cutoff).

These results were obtained with a small prototype system. We aim to achieve a resolution of better than 0.1 pT in the final cryoEDM system. There is still a lot of work to do to achieve this, but the results we have obtained at LSBB mean we are confident we can achieve this.

## 6. Heating pick-up loops to destroy superconductivity

The cryoEDM SQUID system has heaters installed to allow the pick-up loops to be heated into their conducting state so the circulating supercurrent can be destroyed. In our March tests at LSBB we installed a similar heater, consisting of a  $390\Omega$  resistor, on the twisted wire pair between SQUID 3 and its pick-up loop. The twisted wire pair was coiled around the resistor, which was held in a plastic guide of 5 mm diameter, filled with Styrofoam. This was designed to work when submerged in liquid or superfluid helium. When a current of 10 mA was applied to the heater, the input circuit of this SQUID was driven from its superconducting to its normal conducting state. This setup allowed us to study the change in the signals on the other SQUIDs when one loop changed from superconducting to conducting. The result of this experiment is illustrated in figure 17.

When the heater is turned on it creates a magnetic field just like the calibration coil, which is picked up by all three SQUIDs. Unfortunately we cannot measure the magnitude of this signal as it exceeds the slew rate of the SQUIDs (the voltage jump was different each time the heater current was changed, so it appears the SQUIDs were losing flux quanta). SQUID 4 mirrors SQUID 3 to

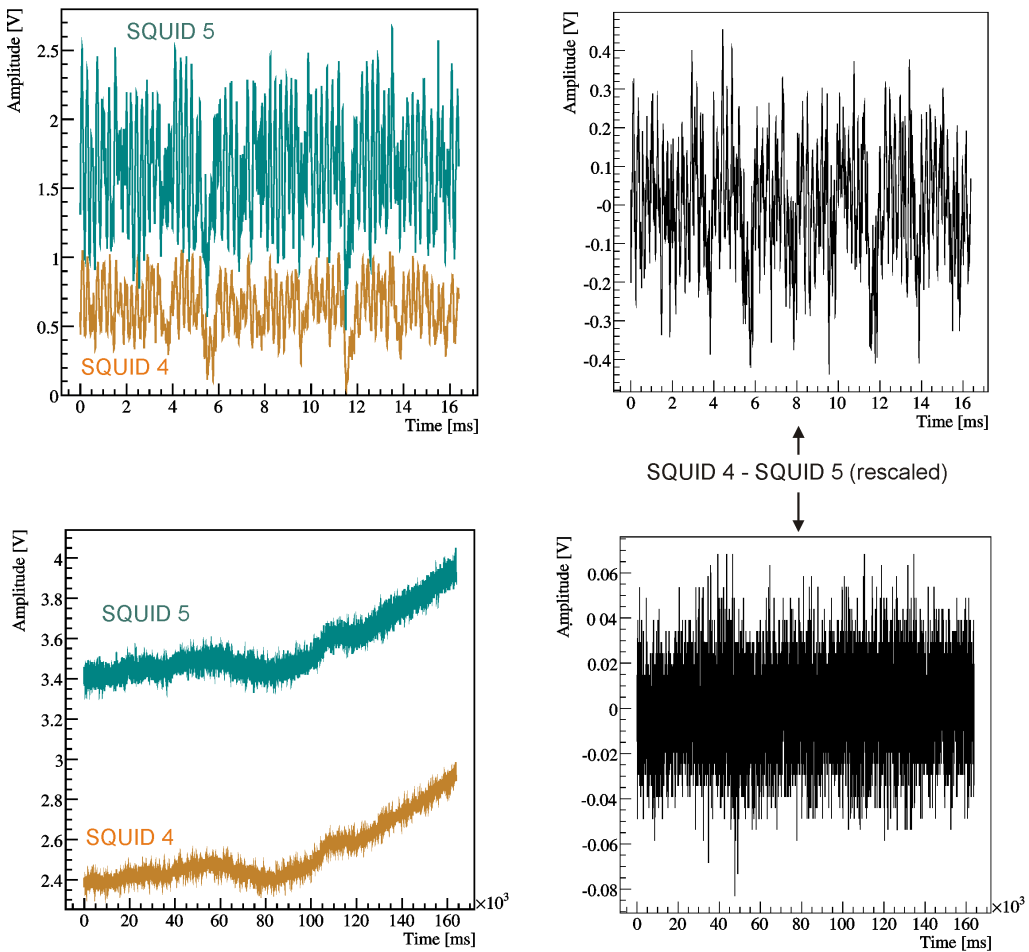


**Figure 16.** Two of the events used to plot the spectra in figure 15. The left hand column shows the signals measured by SQUIDs 4 and 5. The right hand column shows the scaled difference between these two signals. The top row is for an event with a  $1\ \mu\text{s}$  timebase, the bottom row for  $10\ \text{ms}$  timebase. The bit resolution for the transient record was  $\sim 0.01\ \text{V}$ , so the Fourier spectrum of the bottom right hand plot is dominated by quantization noise at the higher frequencies.

an extent as the two pick-up loops are on the same former, but it remains superconducting. SQUID 5 also shows a small shift at the point at which SQUID 3 becomes conducting due to the crosstalk between channels.

One problem with the heater design is that the imperfect twisting of the wires around the heater, leads to the unwanted pick-up of the magnetic field at this point (discussed in section 4.1). In the September setup the twisted wire pair was not coiled tightly, but only wrapped only once around the resistor. However thermal coupling was not so effective, and a current of over  $50\ \text{mA}$  was needed to heat the loop into its conducting state. This required a voltage of  $50\ \text{V}$ , and as the high voltage power supply generated additional noise, no extra experiments with the heater were done during the September run.

In the setup installed in the cryoEDM experiment, we did not want the magnetic field generated

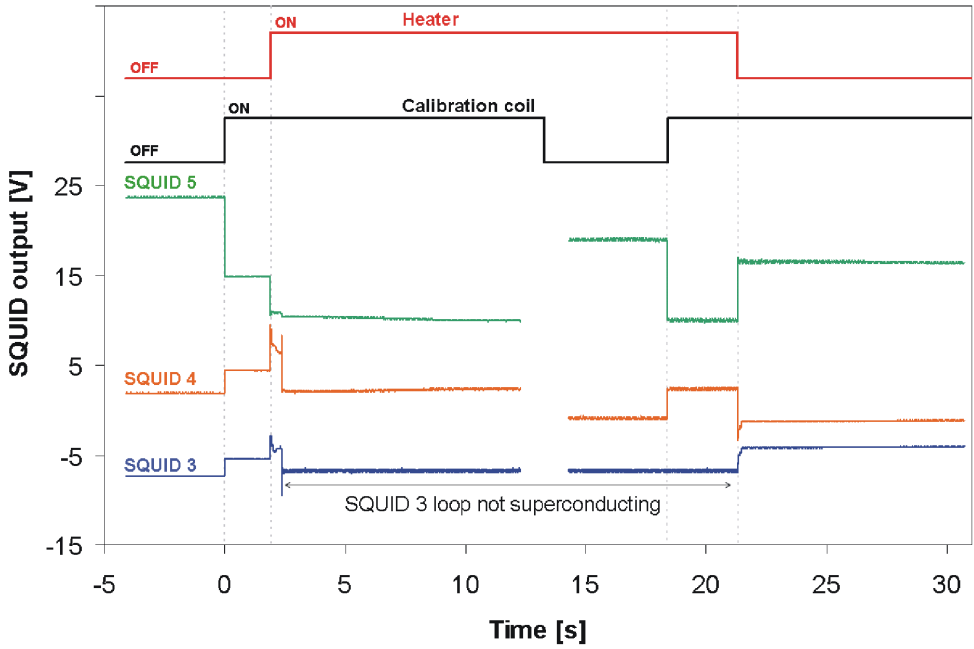


**Figure 17.** The output signal of three SQUIDs (offset for clarity), and the status of the heater and calibration currents as the heater on the loop connected to SQUID 3 was turned on, and then off. The jump at  $t=0$  is due to the calibration coil. At  $t=1.9$  s the heater was turned on, and 0.45 s later the input to SQUID 3 became non-superconducting.

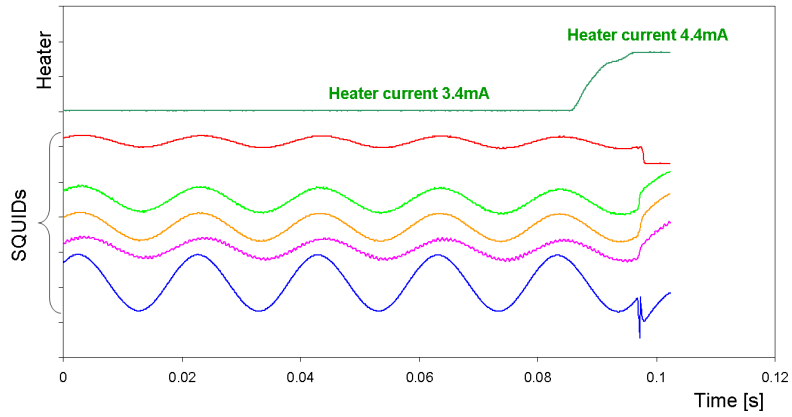


**Figure 18.** The performance of the heater on the cryoEDM SQUID system. This shows the 50 Hz signal measured by five SQUIDs. At 0.086 s the current supply to a heater on the twisted wire pair for one SQUID was increased. At 0.098 s the input circuit of this SQUID becomes conducting. The other SQUIDs record this change of state, but there is no signal on any SQUID before this point, showing that the lead shield around the heater successfully shields the field generated by the heater current.

by the heater to interfere with measurements. Therefore the heater was fixed to the twisted wire pair inside a small lead cylinder, and the wire pair to and from this ran through a superconducting shield made from solder wire with the flux removed. This successfully shielded the wires so we did not pick up any signal when a current was applied to the heater. This is shown in figure 18.

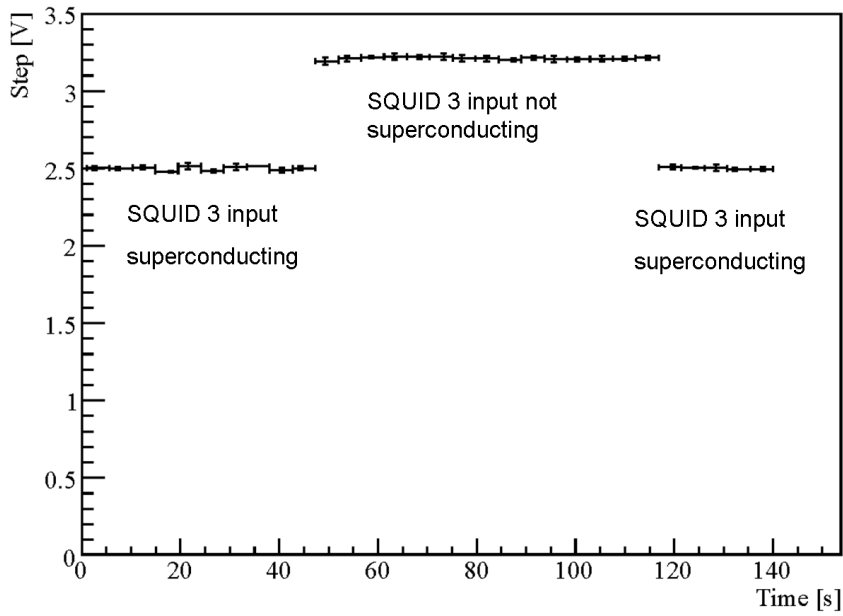


**Figure 19.** The voltage step in SQUID 4 due to the 266 pT signal from the calibration coil, as the heater on SQUID 3 was turned on, then off. The data points have been binned for clarity.

Figure 19 shows the height of the voltage step due to the calibration signal for SQUID 4, plotted against time, as the heater for SQUID 3 was turned on, then off. When SQUID 3 is superconducting, SQUID 4 shows an average jump of 2.5 V. When SQUID 3 becomes conducting, this increases to 3.2 V. This can be explained by considering the crosstalk between the two loops. Loops 3 and 4 are wound on the same former; from equation 4, we can write the change in the flux through loop 4 as

$$\Delta\Phi_4 = 0 = \Delta\Phi_{\text{ext}} + I_4 L_T + I_3 M_{34}. \quad (6.1)$$

When the supercurrent in loop 3,  $I_3$  disappears, the current  $I_4$  in loop 4 must increase so the total flux through the superconducting loop remains constant.

## 7. Conclusions

In this paper we have described a multi-loop SQUID magnetometer we have constructed and tested during two field trips to LSBB in Provence, France. This setup consisted of several parallel pick-up loops connected to the SQUIDs by twisted wire pairs. A calibration coil was installed and one loop had a heater installed on the wire pair to allow it to be heated into its normal conducting state. We have monitored the SQUID output for up to twelve hours and after correcting the effects of SQUID resets and crosstalk between the loops, and calibrating the signal, we compare our measured signal with data from geomagnetic observatories to confirm we have monitored the geomagnetic field.

The primary purpose of these tests was to demonstrate that the prototype cryoEDM SQUID system would function as intended in a suitable environment. We have achieved this objective; and in addition, the project provided an opportunity to develop techniques to extract a useful magnetic field signal from the SQUID output voltage; and to study the interaction between pick-up loops.

We have shown how SQUID resets can be corrected using a simple software algorithm. The crosstalk between channels can be measured from the signal induced on other channels when one SQUID resets, and these figures can be used to correct its effects. A suitably small calibration coil can be modelled as a magnetic dipole allowing us to calibrate our signals to give a final value in nT.

We have examined the variation between channels by rescaling one signal to match another and then taking the difference between these two signals. This scaled difference correlates well with the North-South component of the field measured by geomagnetic observatories, so we conclude the difference is mainly due to pick-up of the horizontal field component.

We have measured a noise level equivalent to a resolution of 0.57 pT over an 80 s measurement time and 10 Hz cut off frequency. Although this is higher than the 0.1 pT resolution we aim to achieve in the cryoEDM apparatus, this is limited by the external geomagnetic field. Our measurements of the noise of a SQUID with no pick-up loop attached suggest we can achieve the desired performance with improved magnetic shielding. We have shown that the frequency spectrum of the scaled difference between the signals measured by two SQUIDs connected to the same pick-up loop does not increase so much at low frequencies as the geomagnetic noise.

Finally we have shown how a suitably designed heater on the twisted-wire-pair between the SQUID and pick-up loop can be used to heat the wire into its normal conducting state (even when used in liquid or superfluid helium). This allowed us to further study the coupling between pick-up loops and show that heating one superconducting loop increased the signal in a parallel loop by 28%. The heater current itself generated a field which was picked-up by other loops; and we have shown how this can be avoided by shielding the heater and twisted pair in lead.

A SQUID magnetometer for cryoEDM has now been installed and successfully tested at the ILL in Grenoble, however as expected, all measurements to date have been limited by the electromagnetic environment. We are working on improving this with better shielding.

## Acknowledgments

We would like to thank everyone at LSBB for their excellent hospitality; and allowing us to record the signal from their magnetometer together with ours. We thank the geomagnetic observatories mentioned and INTERMAGNET for publishing their data. We also thank Jim Grozier for numerical modelling of the calibration coil. This work was funded through PPARC and the EC IHP network HPRN-CT-2002-00322 on Applied Cryodetectors.

## References

- [1] Rutherford Appleton Laboratory, Particle Physics Department, *Particle Physics Experiments Report 2002*, pg. 1–5, RAL-TR-2003-006.
- [2] P.G. Harris et al., *New Experimental Limit on the Electric Dipole Moment of the Neutron*, *Phys. Rev. Lett.* **82** (1999) 904.
- [3] C.A. Baker et al., *Improved Experimental Limit on the Electric Dipole Moment of the Neutron*, *Phys. Rev. Lett.* **97** (2006) 131801.
- [4] K. Green et al., *Performance of an atomic mercury magnetometer in the neutron EDM experiment*, *Nucl. Instrum. Meth. A* **404** (1998) 381.

- [5] C.A. Baker et al., *Experimental measurement of ultracold neutron production in superfluid  $^4\text{He}$* , *Phys. Lett. A* **308** (2003) 67.
- [6] M.A. Espy, A. Matlashov, R.H.Jr. Kraus, P. Ruminer, M. Cooper and S. Lamoreaux, *SQUIDS as detectors in a new experiment to measure the neutron electric dipole moment*, *IEEE Trans. Appl. Supercond.* **9** (1999) 3696.
- [7] F. Wellstood, C. Heiden and J. Clarke, *Integrated dc SQUID magnetometer with a high slew rate*, *Rev. Sci. Instrum.* **55** (1984) 952.
- [8] G. Waysand, D. Bloyet, J.P. Bongiraud, J.I. Collar, C. Dolabdjian and Ph. Le Thiec, *First characterization of the ultra-shielded chamber in the low-noise underground laboratory (LSBB) of Rustrel-Pays d'Apt*, *Nucl. Instrum. Meth. A* **444** (2000) 336.
- [9] G. Waysand et al., *Seismo-Ionosphere Detection by Underground SQUID in Low-Noise Environment in LSBB-Rustrel, France*, to be published in *European Physical Journal of Applied Physics*.
- [10] J. Clarke and A.I. Braginski, *The SQUID Handbook*, Wiley-VCH, Berlin (2004) [ISBN: 3527404082].
- [11] H.J.M. ter Brake, H.J.M. ter Brake, F.H. Fleuren, J.A. Ulfrnan and J. Flokstra, *Elimination of flux-transformer crosstalk in multichannel SQUID magnetometers*, *Cryogenics* **26** (1986) 667.
- [12] M.T. Thompson, *Inductance calculation techniques*, in *Power Control and Intelligent Motion*, December 1999, [http://www.classictesla.com/download/indu\\_pt\\_2.pdf](http://www.classictesla.com/download/indu_pt_2.pdf).
- [13] INTERMAGNET, <http://www.intermagnet.org>.
- [14] J.J. Love, *Magnetic monitoring of earth and space*, *Phys. Today* **61** (2008) 31.
- [15] <http://lsbb.unice.fr/caracteristiques.htm> (in French).